Clays and Clay Minerals, Vol. 65, No. 5, 355–366, 2017.

THE SOLID-STATE CONVERSION OF KAOLIN TO $KAlSiO_4$ MINERALS: THE EFFECTS OF TIME AND TEMPERATURE

DANIELA NOVEMBRE[1] AND DOMINGO GIMENO[2]

[1] Dipartimento di Ingegneria e Geologia, Università degli Studi "G. D'Annunzio" Via dei Vestini 30, 66013 Chieti, Italy
[2] Departamento de Geoquimica, Petrologia i Prospecció Geologica, Universitat de Barcelona, 08028 Barcelona, Spain

Abstract—In recent years $KAlSiO_4$ polymorphs have become minerals of interest from an industrial point of view; they have various applications in technological and medical fields. The costs of synthesis processes are often significant and so, in the present study, an attempt was made to develop a new synthesis protocol using a widely available and inexpensive, natural starting material. The $KAlSiO_4$ polymorphs synthesized here were kalsilite and $KAlSiO_4$-01 – 01 refers to the high-temperature polymorph of $KAlSiO_4$ (Cook *et al.*, 1997; Gregorkiewitz *et al.*, 2008; Kremenovic *et al.*, 2013). $KAlSiO_4$ polymorphs were synthesized using kaolin; the effects of time and temperature on the synthesis process were investigated. A solid-state synthesis protocol was developed which required the mixing of the calcined kaolin with K_2CO_3 in stoichiometric proportions at temperatures of 700 and 800ºC at atmospheric pressure. Crystallization of kalsilite at 700ºC was demonstrated while that of $KAlSiO_4$-01 was revealed at 800ºC. Synthetic kaliophilite H2 was found in both of the experiments as a metastable phase. The products of synthesis were characterized by powder X-ray diffraction (XRD), scanning electron microscopy (SEM), inductively coupled plasma optical emission spectrometry (ICP-OES), infrared spectroscopy (IR), and ^{29}Si magic-angle spinning solid-state nuclear magnetic resonance spectroscopy (^{29}Si MAS NMR). Calculation of cell parameters (through Rietveld refinement) and the density and specific surface area of the phases synthesized was also achieved. The amount of amorphous phase in the synthesis powders was estimated by means of quantitative phase analysis using the combined Rietveld and reference intensity ratio methods. In particular, the results of the spectroscopic, chemical, and morphological characterizations are in agreement with the data available for these minerals in the literature, thus confirming the effectiveness of the experimental protocol. The quantitative phase analysis (QPA) also indicated the high purity of the powders synthesized, thus allowing for industrial applications.

Key Words—ICP-OES, IR, Kaliophilite, Kalsilite, Kaolinite, SEM, ^{29}Si MAS NMR, Solid-state Synthesis, XRD.

INTRODUCTION

A detailed review of the several polymorphic forms of $KAlSiO_4$ that have been recognized and refined structurally in the past was given by Okamoto (1997). One of the polymorphs is represented by low kalsilite (*P*63), a room-temperature variant of stuffed trydimite, the structure of which was first refined (Perrotta and Smith, 1965) with a = 5.16 and c = 8.69 Å; low kalsilite was synthesized (Andou and Kawahara, 1984) under hydrothermal conditions (600ºC, 15 days) with hexagonal symmetry (a = 5.15; c = 8.69); low kalsilite was later synthesized also by Okamoto (1997) (600ºC, 14 days), who observed its modifications at high temperature (>865ºC) in the high kalsilite polymorph which is also hexagonal (*P*63*mc* or *P*63/*mmc*). This point was also investigated by Kawahara *et al.* (1987) and the structural change was fixed at 865ºC.

Another high-temperature polymorph is represented by $KAlSiO_4$-01, first synthesized by Cook *et al.* (1997) and refined as having orthorhombic symmetry in the space group *P*21212 and refined further by Gregorkiewitz *et al.* (2008) as being the space group $P12_11$. More recently, the structure of single crystals of $KAlSiO_4$-01 in the monoclinic system was resolved by Kremenovic *et al.* (2013) ($P2_1$). The transformations of $KAlSiO_4$-01 into the polymorph $KAlSiO_4$-02 at temperatures of >1450ºC were investigated by Cook *et al.* (1997).

Another polymorph known as "synthetic kaliophilite" was synthesized by Tuttle and Smith (1958) and later named "kaliophilite H_2" by Merlino (1984). The structure was refined (Okamoto and Kawahara, 1996; Okamoto, 1997) as having hexagonal symmetry (*P*63*mc*) with a = 5.17 and c = 8.49 Å.

Due to their framework structure of linked (Si,Al)O4 tetrahedra, $KAlSiO_4$ plymorphs are, in fact, very versatile minerals finding applications in various industrial fields. The application of kalsilite as a cement in restorative dentistry has been explored in the recent past (Liou *et al*., 1994; Zhang *et al.*, 2007). During the preparation of aluminosilicate glass-ceramics, multiphase products (*e.g.* kalsilite, leucite, and sanidine) are often produced, according to Bogdanoviciene *et al.* (2008). More recently, kalsilite was used as a heterogeneous catalyst for transesterification of soybean oil

* E-mail address of corresponding author:
daniela.novembre@unich.it
DOI: 10.1346/CCMN.2017.064077

with methanol to biodiesel (Wen *et al.*, 2010). High thermal-expansion ceramics have been prepared from $KAlSiO_4$-01 for bonding on copper or silver (Ota *et al.*, 1996). The material is very important in terms of high-temperature technologies (Gregorkievitz *et al.*, 2008) as has been found in blast-furnace linings (Rigby and Richardson, 1947), magnetohydrodynamic generators (Cook *et al.*, 1977), and hazardous-waste incinerator clinkers (Li *et al.*, 2003).

The synthesis of $KAlSiO_4$ polymorphs was achieved in the past by various methods: Cation exchange from nepheline (Dollase and Freeborn, 1977); the sol-gel method using TEOS (tetraethoxysilane, $Si(OH)_4$) (Hamilton and Henderson, 1968) or hydrated SiO_2, CH_3COOH, and $Al(NO_3)_3{\cdot}9H_2O$ (Bogdanovicieni *et al.*, 2007); hydrothermal methods (Smith and Tuttle, 1957; Kopp *et al.*, 1961; Andou and Kawahara, 1984; Okamoto and Kawahara, 1996; Okamoto, 1997; Becerro *et al.*, 2009; Becerro and Mantovani, 2009); the flux technique (Kremenovicic *et al.*, 2013); and solid-state synthesis from zeolite, silicate compounds, and kaolinite (Dimitrijevic and Dondur, 1995; Kosanović *et al*., 1997; Heller-Kallai and Lapides, 2003). The reactions of kaolinite at elevated temperatures have found many applications in the past; several studies have focused, in particular, on the reactivity of metakaolinite with alkali solutions in successful synthesis of zeolite (Gualtieri *et al.*, 1997; Akolekar *et al.*, 1997; Demortier *et al.*, 1999; Sanhueza *et al.*, 1999; Zhao *et al.*, 2004; Heller-Kallai and Lapides, 2007; Ríos *et al.*, 2009; Novembre *et al.*, 2005, 2011) or in the synthesis of kalsilite (Becerro and Mantovani, 2009; Novembre *et al.*, 2017b).

As far as the solid-state method is concerned, the pioneering work was done by Gorgeu (1887) who mixed metakaolin with potassium carbonate leading to the formation of a crystalline salt such as kaliophilite. Synthesis of $KAlSiO_4$ minerals using kaolinite as the starting material has been explored under modern laboratory conditions by Heller-Kallai and Lapides (2003) only; the thermal reactions of kaolinite with potassium carbonate was explored by those authors at 700ºC for 1 h, yielding synthetic kaliophilite as the final product. No characterization of the products synthesized is available from those authors, nor, in fact, was any investigation of the phase transitions of the "metastable" phase obtained, kaliophilite (*sensu* Tuttle and Smith, 1958), made known.

The aim of the present study was to synthesize minerals with the formula $KAlSiO_4$ using kaolin as the starting material and to study the effects of time and temperature on the crystallization times and stability field of the minerals obtained. In particular, the thermal reaction of kaolinite with potassium carbonate during a certain time interval was of interest in terms of establishing which are the metastable and which are the stable phases and to provide full characterization of the phases synthesized with a view to possible industrial applications.

EXPERIMENTAL

Materials and reagents

The kaolin sample used in the present study was Standard Porcelain from IMERYS Minerals Ltd (Cornwall, UK). For the chemical composition of kaolin and its mineralogical characterization, see Novembre *et al.* (2011). Preliminary calcination of kaolin was carried out using the following procedure: aliquots of kaolin were placed in open porcelain crucibles which were heated in a Gefran Model 1200 furnace (Gefran Spa, Brescia, Italy) to the calcination temperature (650ºC) at a pressure of 1 atm. The heating rate of the sample was 1.5ºC s^{-1}. Once the calcination temperature was reached, the crucibles were left in the furnace for 2 h and then removed and cooled at room temperature.

The K_2CO_3 used in the synthesis protocol was purchased from Riedel-de Haën (Honeywell Riedel-de Haën, Bucharest, Romania). The purity of the reagent was $\geqslant$99%.

Syntheses

Two synthesis runs were performed by the mixing of calcined kaolinite (4 g) with K_2CO_3 (4 g) at 700 or 800ºC (Table 1). Powders, finely mixed, were placed inside porcelain crucibles in a muffle furnace and held at a fixed temperature (700 or 800ºC) and ambient pressure. During the periodic sampling, a loss of mass in the open crucible was observed (Novembre *et al.*, 2010; Pasculli and Novembre, 2012) and attributed to CO_2 diffusion through the granular material contained in the crucible.

Techniques

The synthesis products were analysed by Powder X-ray diffraction (PXRD, Siemens D5000, Siemens-

Table 1. Starting-mixture compositions and mineralogical assemblages obtained from experimental runs.

Synthesis run	Temperature (ºC)	Starting mixture	Mineralogical assemblage
1	700	4 g metakaolinite + 4 g K_2CO_3	2–24 h: kaliophilite H2 + kalsilite 10 days: kalsilite
2	800	4 g metakaolinite + 4 g K_2CO_3	1–5 h: kaliophilite H2; 5 days: $KAlSiO_4$-01

Bruker, Billerica, Massachussetts, USA) operating with Bragg-Brentano geometry; CuKα = 1.518 Å, 40 kV, 40 mA, 4–45º2θ scanning interval, step size of 0.020º2θ. Samples collected periodically were analyzed by PXRD; samples, collected at other time intervals, were washed thoroughly with distilled water and oven dried at 40ºC for 24 h. The powder samples were prepared as smears on glass slides; identification of $KAlSiO_4$ polymorphs and relative peak assignments were performed with reference to the following JCPDS codes: 00-011-0579 for kalsilite; 00-018-0987 for $KAlSiO_4$-01; and 00-011-0313 for kaliophilite H2. Both the crystalline and amorphous phases in the synthesis powders were estimated using QPA, applying the combined Rietveld and reference intensity ratio (RIR) methods; corundum NIST-SRM676a (National Institute of Standards and Technology – Standard Reference Material, U.S. Department of Commerce, Gaithersburg, Maryland, USA) was added to each sample, making up 10% of each (according to the strategy proposed by Gualtieri, 2000), and the powder mixtures were homogenized by hand grinding in an agate mortar. Data for the QPA refinement were collected over the angular range 5–120º2θ with steps of 0.02º2θ and 10 s $step^{-1}$, a divergence slit of 0.5º, and a receiving slit of 0.1 mm.

Data were processed using the *GSAS* software (Larson and Von Dreele, 1997) and the graphical interface *EXPGUI* (Toby, 2001). The unit-cell parameters were determined, starting with the structural models proposed by Kremenovic *et al.* (2013) for $KAlSiO_4$-01 and by Andou and Kawahara (1984) for kalsilite. The refined parameters were background parameters, zero shift, cell parameters, and peak profiles.

IR studies of the products synthesized were conducted with an FTLA2000 spectrometer (ABB Analytical, Quebec, Canada), served by a KBr beam splitter and a deuterated triglycine sulfate (DTGS) detector; the source of IR radiation was a SiC (Globar) filament. The samples were treated according to the method of Robert *et al.* (1989) using powder pressed pellets (sample:KBr ratio of 1/100 and pellitization pressure of 15 t/cm^2); spectra were acquired with 64 scans and processed with the program *GRAMS-AI*™ (Thermo Fisher Scientific, Waltham, Massachusetts, USA).

^{29}Si MAS NMR was performed using a Bruker Advance-Spectrospin 300 MHz instrument (Bruker, Billerica, Massachusetts, USA) (speed of rotation at the magic angle of 4000 Hz, variable number of scans from 100 to 200–400, and pulse length (90º) p1 = 8 μs, and scanning time t1 = 5 s. The spectra were processed using the program *WINNMR* from Bruker. The chemical shifts were referenced to trimethylsilyl propionic (2,2,3,3)-d_4 acid, sodium salt TSP (Sigma Aldrich, St. Louis, Missouri, USA) for ^{29}Si.

The SEM analyses were carried out using a JEOL JSM-840 instrument (JEOL, Akishima, Tokyo, Japan) operating at 15 kV and with window conditions ranging from 18 to 22 mm, following the procedure outlined by Ruggieri *et al.* (2011).

ICP-OES analysis of synthesized powders was carried out using a Perkin Elmer Optima 3200 RL (Perkin Elmer Corporation, Waltham, Massachusetts, USA), following the procedure and analytical error range as explained by Fernandez-Turiel *et al.* (2003) and references therein, *i.e.* the analytical quality assurance was performed using replicate samples, triplicate measuring of each sample analyzed by ICP-MS (ICP mass spectrometry), internal calibration using ^{115}I. Sample preparation was by means of prior alkaline fusion in and subsequent acid solubilization as explained by Aulinas *et al.* (2010).

The density of kalsilite and $KAlSiO_4$-01 was calculated by He-picnometry using an AccuPyc 1330 pycnometer (Micromeritics Instrument Corporation, Norcross, Georgia, USA).

Differential thermal analysis (DTA) and thermogravimetry (TG) were performed on raw kaolin using a Mettler TGA/SDTA851e instrument (10º/min, 30–1100ºC, sample mass of ~10 mg, Al_2O_3 crucible) (Mettler Toledo, Greifensee, Switzerland), as explained by Novembre *et al.* (2014).

RESULTS AND DISCUSSION

Characterization of the starting material

Morphological (SEM), thermal (DTA-TG), and spectroscopic (IR and ^{29}Si MAS-NMR) characterizations of kaolin were performed. The morphological analysis showed that the kaolinite particles had an irregular shape and were up to micrometers long (Figure 1).

Thermal analysis (Figure 2) revealed the typical endothermic and exothermic peaks of kaolin with a continuous water loss between 29 and 998ºC. Two

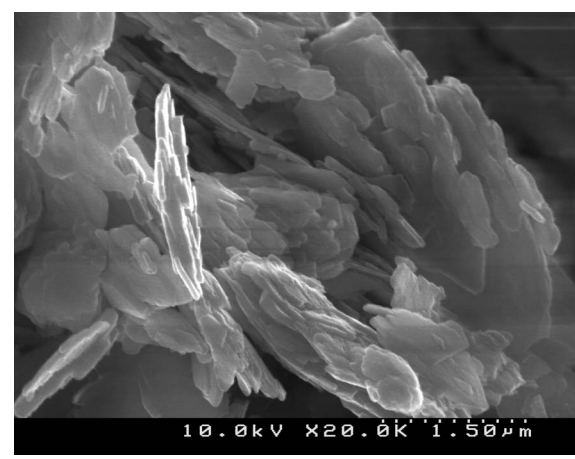

Figure 1. SEM image of raw kaolin.

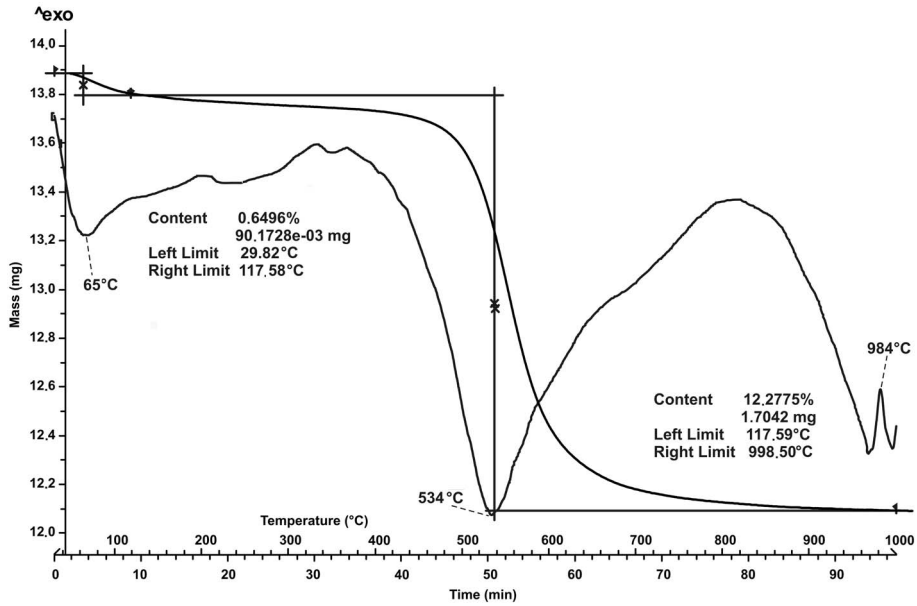

Figure 2. DTA and TG analysis of raw kaolin.

endothermic peaks were observed; the first at 65ºC was related to the loss of adsorbed water and the second at 534ºC was ascribed to the dehydroxylation of kaolinite. An exothermic peak was found at ~780ºC and is related to the disruption of the kaolinitic structure. The exothermic peak located at 984ºC is due to the formation of the Al-Si spinel phase from kaolinite. Two different steps in the loss of water were observed; the first ranging between 29 and 117ºC and the second between 117 and 998ºC. The total mass loss was 1.71 mg corresponding to a starting water content of 12%.

Infrared analysis was conducted on kaolin raw material (Figure 3). The bands between 3750 and 3500 cm^{-1} are attributed to OH stretching. Five bands, in particular, were noted at 3648, 3653, 3667, 3674, and 3686 cm^{-1}, and related to the inner surface –OH in phase/out-of-phase stretching vibrations (Cheng *et al.*, 2010a; Frost *et al.*, 2001b); a band located at 3619 cm^{-1} is related to the inner –OH stretching vibration (Cheng *et al.*, 2010a; Frost *et al.*, 2001b). In the lower-wavenumber region of the IR spectra (1800–400 cm^{-1}) a band at 1113 cm^{-1} was revealed

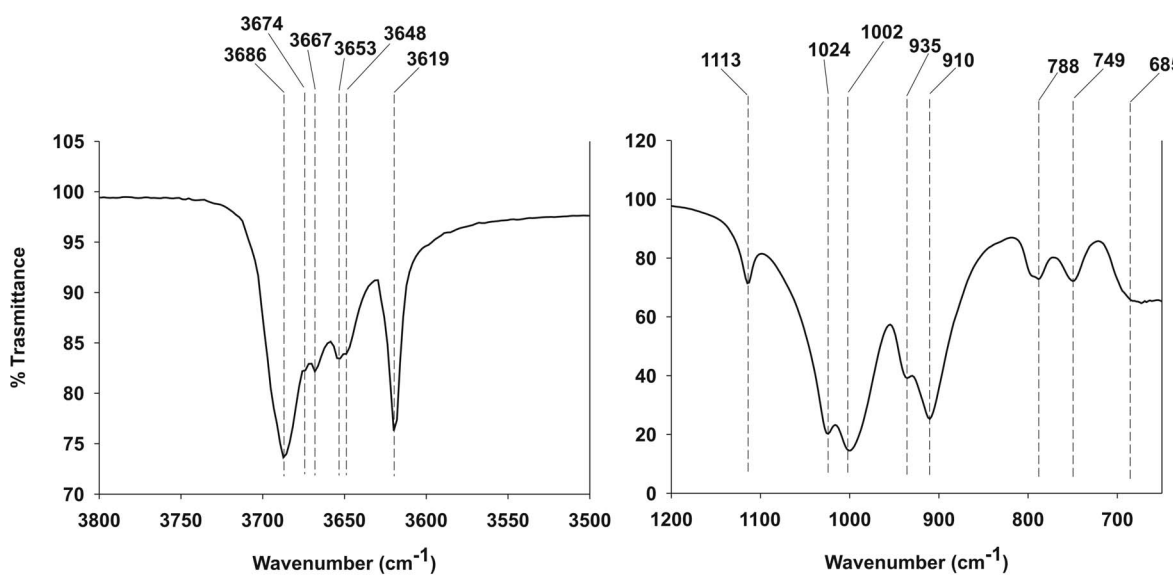

Figure 3. IR spectra of raw kaolin.

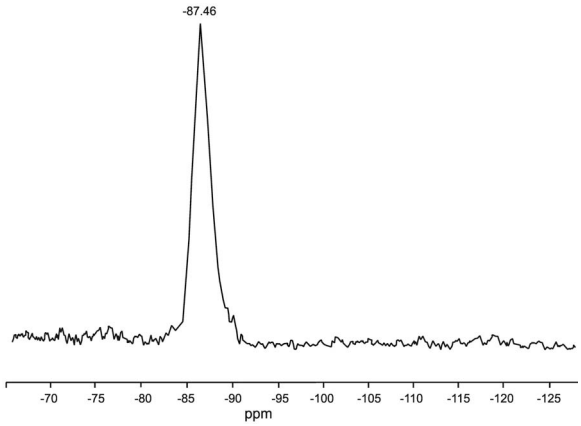

Figure 4. ^{29}Si MAS-NMR spectrum of raw kaolin.

and attributed to apical Si−O stretching vibrations (Cheng *et al.*, 2010b); in the same wavenumber region, two bands located at 1024 and 1002 cm^{-1} were noted and are related to apical Si−O stretching vibrations (Cheng *et al.*, 2010b); two other bands at 935 and 910 cm^{-1} are attributed to Al−OH bending vibrations (Qtaitat and Al-Trawneh, 2005); three bands at 788, 749, and 685 cm^{-1} are related to −OH (Al-OH) translational vibrations (Frost *et al.*, 2001a).

The ^{29}Si MAS-NMR spectrum of kaolin (Figure 4) reveals a peak located at −87.46, the position of which is consistent with the data of Ríos and Williams (2010).

Mineralogical, crystallographic, and chemical characterization of synthetic products

The results of PXRD analyses conducted on samples of the two experimental runs (Figures 5, 6; Table 1) revealed interesting phases and phase transitions. In synthesis run 1 (Figure 5) the crystallization of synthetic kaliophilite H2 as a metastable phase (*sensu* Tuttle and Smith, 1958) is shown together with kalsilite in the run lasting 2−24 h; after this, kaliophilite H2 became unstable and kalsilite was the only phase remaining after 10 days.

In synthesis run 2 (Figure 6), kaliophilite H2 was the first phase to occur in the synthesis run lasting 2−5 h; after this, kaliophilite H2 became unstable and $KAlSiO_4$-01 was the only phase remaining after 5 days.

This temporal synthesis trend can be read in two ways. (1) From an industrial point of view, it offers the possibility of an economic synthesis of both products. (2) From a strictly geological point of view, kalsilite has been reported as a magmatic product in some rare volcanic environments. The present result seems to indicate, however, that the pyrometamorphic genesis of both is viable in terms of the short time of magma-chamber residence, at least in terms of a direct relationship of alkaline basaltic magma (especially if K-rich magmas are involved) by digestion of tonstein-like sedimentary xenoliths (for a discussion on pyrometamorphism associated with basaltic rocks and products,

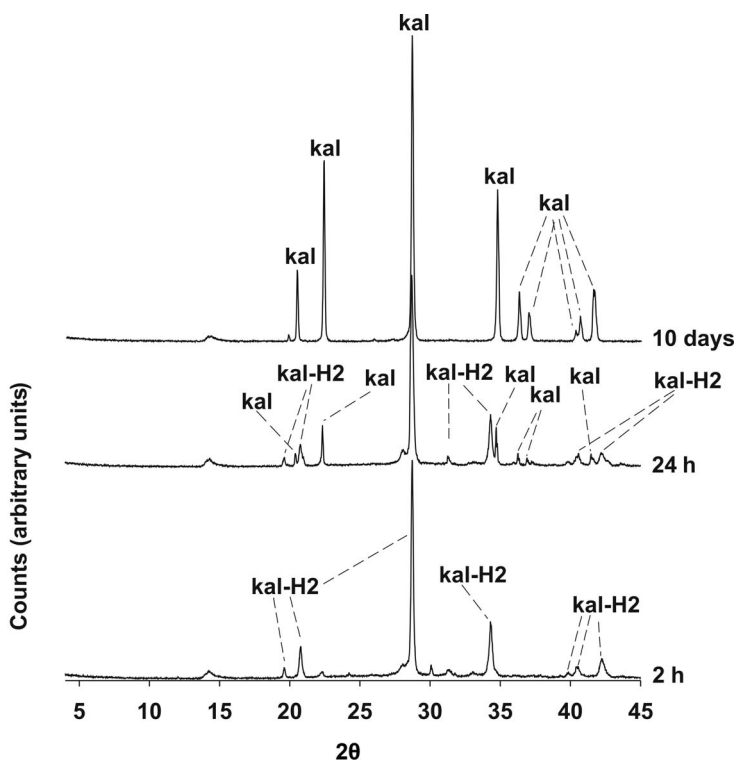

Figure 5. PXRD sequence of synthesis run 1. Kal-H2: kaliophilite H2; Kal: kalsilite.

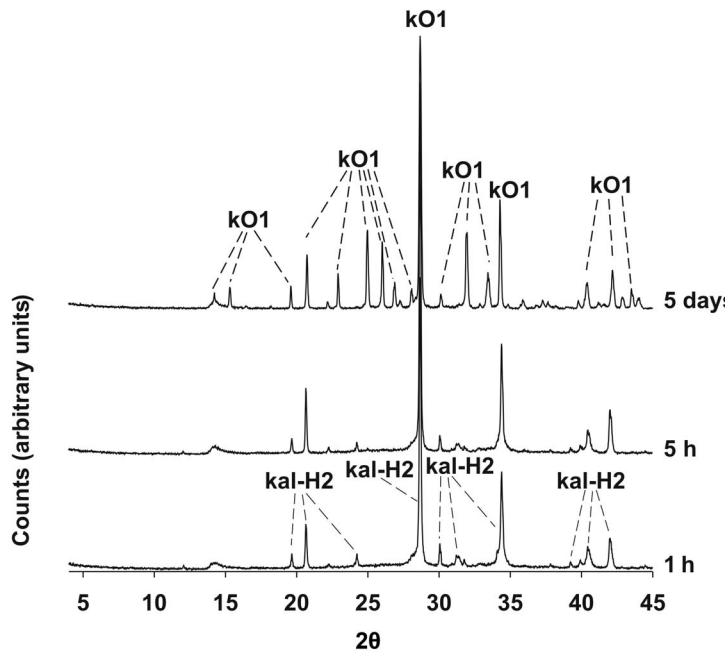

Figure 6. PXRD sequence of synthesis run 2. Kal-H2: kaliophilite H2; KO1: $KAlSiO_4$-01.

see the study by Sabine and Young (1975) and by Novembre *et al.* (2017a), and references therein).

The end-products of syntheses 1 and 2, consisting of monomineralic powders of kalsilite and $KAlSiO_4$-01, respectively, were considered for further characterizations.

The observed and calculated (Rietveld refinement) profiles and difference plot (Figure 7) for kalsilite and $KAlSiO_4$-01, each mixed with corundum NIST 676a, were obtained for the end run samples of synthesis runs 1 and 2 (Figure 7a,b, respectively). (Corundum was added in order to perform the QPA analysis; this is a procedure in which a known amount of corundum NIST 674*a* or 676*a*, is added to the mixture (10 wt.%) and considered as a component itself. The refined values of the Rietveld phase fractions are converted into weight fractions and rescaled into absolute values with respect to the amount of added spike.) The cell parameters for kalsilite, having hexagonal symmetry (space group $P6_3$) were calculated from the Rietveld refinement (Table 2) and were $a_0 = b_0 = 5.1652$ (0.00053) Å and $c_0 = 8.6894$ (0.00069) Å; the cell parameters of $KAlSiO_4$-01, refined as having monoclinic symmetry, space group $P2_1$, were $a_0 = 15.67871$(0.00437) Å, $b_0 = 9.06004$(0.00217) Å, and $c_0 = 8.56471$(0.00427) Å.

When comparing the refined cell parameters with bibliographic data, good agreement with values proposed for kalsilite by Andou and Kawahara (1984) and for $KAlSiO_4$-01 by Kremenovic *et al.* (2013) was achieved.

The results of the QPA analysis (Table 2) indicated that the calculated amount of amorphous phase in the sample after 10 days of synthesis in run 1 was 6.6(9)%, thus resulting in a final product of 93.4(9)% kalsilite; the calculated amorphous phase in the sample at 5 days of synthesis in run 2 was 6.5(8)%, thus resulting in a final product of 93.5(8)% $KAlSiO_4$-01.

The results of chemical analyses of the samples of kalsilite (after 10 days of synthesis in run 1) and of $KAlSiO_4$-01 (after 5 days of synthesis in run 2) and Si/(Si+Al) ratios are shown in Table 3. The chemical formulae of kalsilite and $KAlSiO_4$-01 were calculated based on the chemical analysis results reported in Table 3: $(K_{8.01})(Al_{7.98}Si_{8.01})O_{32}$ and $(K_{6.98})(Al_{8.03}Si_{8.23})O_{32}$, respectively.

Morphological and physical characterization

The SEM image (Figure 8a) of the sample of synthesis run 1 at 10 days provides evidence of the crystalline growth of hexagonal crystals of kalsilite, the maximum axis of which measured 4.5 μm; powder of synthesis run 2 at 5 days (Figure 8b) indicated the presence of a plate-like prismatic habit of $KAlSiO_4$-01 with an average length of 4 μm.

Density values of 2.624 (0.05) and 2.611(0.02) g/cm^3 (Table 4) were calculated for $KAlSiO_4$-01 and kalsilite, respectively, which are comparable to those obtained by Gregorkievitz *et al.* (2008), Kremenović *et al.* (2013), and Hokamoto (1997).

IR and ^{29}Si MAS NMR

The IR spectra of kalsilite and $KAlSiO_4$-01 from both of the synthesis runs (Figures 9, 10), along with the assignments for the absorption bands (Table 5), were analyzed in the context of known data for kalsilite (Becerro *et al.*, 2009; Henderson and Taylor, 1988) and for $KAlSiO_4$-01 (Dimitrijevic and Dondur, 1995).

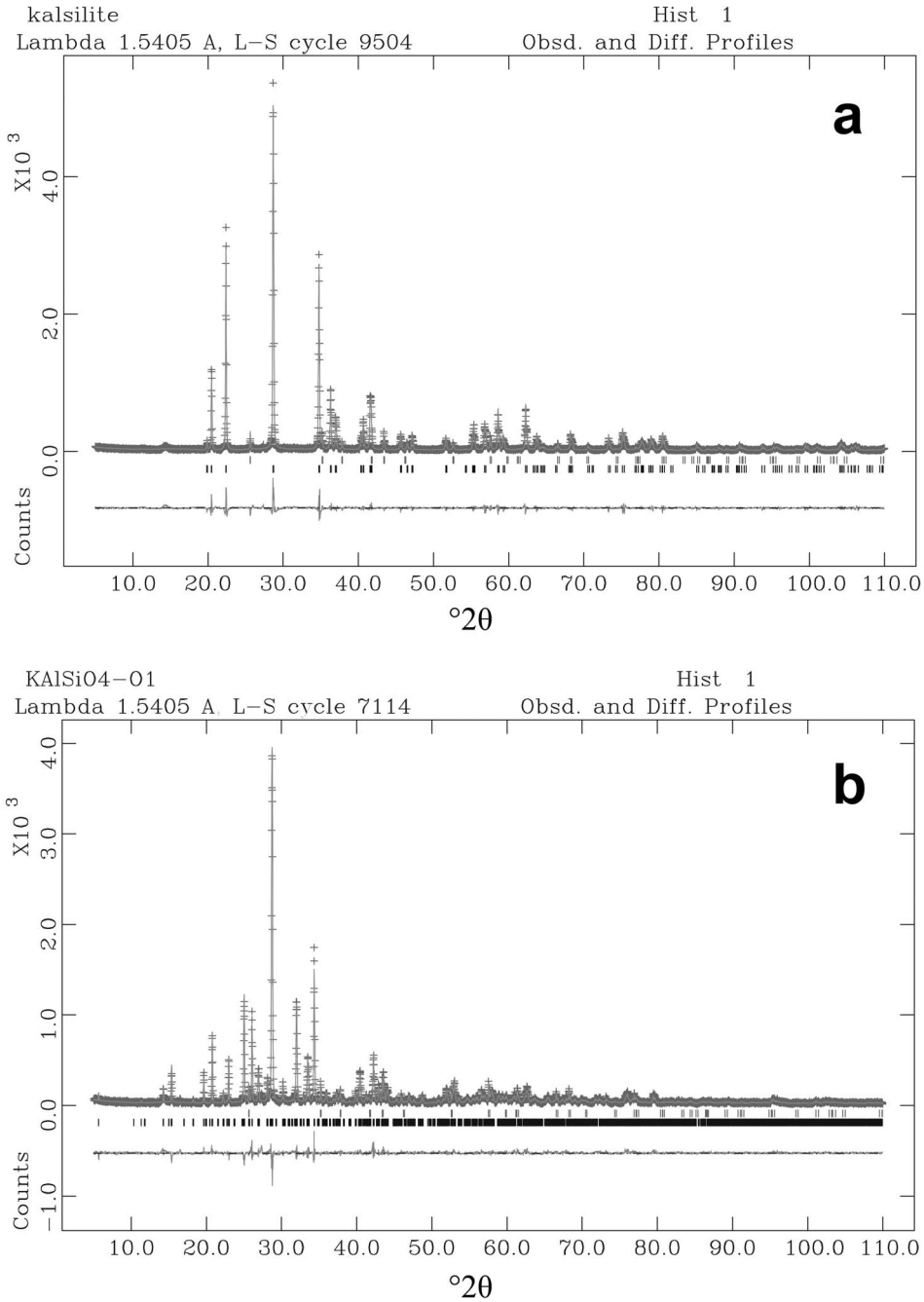

Figure 7. Rietveld refinement plots: observed (+) and calculated profiles (solid lines) and difference plots for: (a) kalsilite + corundum NIST 676a; and (b) $KAlSiO_4$-01 + corundum NIST 676a. The tick marks show the positions of the Bragg peaks.

For kalsilite, a single band was noted in the region of the asymmetric Si−O stretch, located at 966 cm^{-1}; a minor band associated with symmetric Si−O stretch vibrations was observed at 685 cm^{-1}.

For $KAlSiO_4$-01, eight bands were found in the asymmetric Si−O stretch region located at 1106, 1071, 1034, 988, 973, 959, 941, and 930 cm^{-1}, respectively. Two bands related to symmetric Si−O stretching were located at 693 and 663 cm^{-1}.

The ^{29}Si MAS-NMR spectrum of kalsilite revealed a single peak at −88.9 ppm corresponding to the Si type of environment Q^4 (4Al) (Figure 11a, Table 6). The data are consistent with values reported for this mineral by Becerro *et al.* (2009) for a kalsilte synthesized under hydrothermal conditions using kaolinite as the starting material; good agreement was also found with the data of Dimitrijevic and Dondur (1995) for a kalsilite obtained by cationic exchange on zeolite LTA. As

Table 2. Rietveld refinement of samples at 10 days of synthesis in run 1 and 5 days of synthesis in run 2: experimental conditions and crystallographic data for kalsilite and $KAlSiO_4$-01 plus 10% corundum NIST 676a. The results of the QPA analyses of kalsilite and $KAlSiO_4$-01 in each sample are reported as percentages of the amorphous component. Wavelength (Å): CuKα of the X-ray tube.

Sample	10 days, synthesis run 1 + 10% Corundum NIST 676a	5 days, synthesis run 2 + 10% Corundum NIST 676a
Wavelength (Å)	1.5418	1.5418
No. of observations	9504	7114
R_{wp}	0.18	0.15
R_p	0.13	0.11
CHI^2	2.37	1.75
% amorphous	6.6(9)	6.5(8)
% phase kalsilite	93.4(9)	
% phase $KAlSiO_4$-01		93.5(8)
Space-group kalsilite	$P6_3$	
a (Å)	5.1652(0.00053)	
b (Å)	5.1652(0.00053)	
c (Å)	8.6894(0.00069)	
Space-group $KAlSiO_4$-01		$P2_1$
a (Å)		15.6787(0.00437)
b (Å)		9.0600(0.00217)
c (Å)		8.5647(0.00427)

Table 3. Chemical characterization of products of synthesis in runs 1 and 2. Values for the MgO, MnO, TiO_2, and P_2O_5 oxides were below their respective detection limits (*) (Stebbins *et al.*, 1986).

Temperature (ºC)	K_2O (%)	SiO_2 (%)	Al_2O_3 (%)	Time (h)	PXRD
700	29.75	37.95	32.10	30	kalsilite
(*)	28.50	39.3	31.60		
800	26.62	40.01	33.15	20	$KAlSiO_4$-01
(*)	26.00	40.60	32.10		

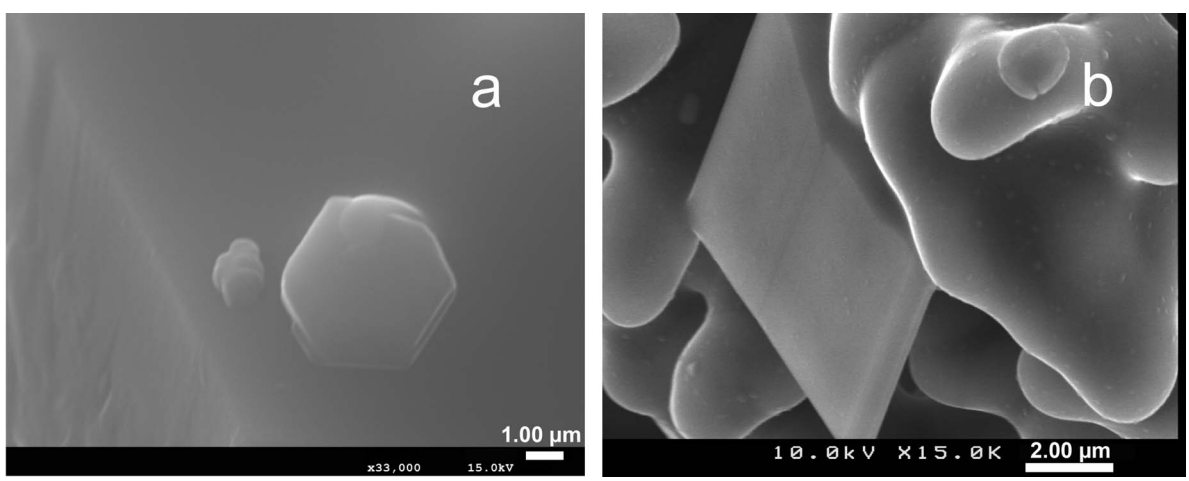

Figure 8. SEM images of kalsilite synthesized at 10 days of synthesis in run 1 (a) and of $KAlSiO_4$-01 crystals synthesized at 5 days of synthesis in run 2 (b).

Table 4. Density analysis of the mineral phases.

Sample	Density g/cm^3
$KAlSiO_4$-01 (5 days) 800ºC	3
(*)	2.57
(**)	3
Kalsilite (10 days) 700ºC	3
(***)	2.64

*Gregorkievitz *et al.* (2008); **Kremenovic *et al.* (2013), and ***Hokamoto (1997).

noted by Becerro *et al.* (2009), an additional peak attributed to Q^3 (3Al) was reported for kalsilites by Stebbins *et al.* (1986) and by Hovis *et al.* (1992), who obtained them by cationic exchange on plutonic nephelines, and who interpreted it as being a result of silica content in excess of the ideal 1:1 Si/Al ratio. The absence of this peak in the sample synthesized in the present study is consistent with a 1:1 Si/Al ratio, thus resulting in complete Si/Al order in the kalsilite sample of synthesis run 1.

For $KAlSiO_4$-01 the sample at 20 h of synthesis in run 2 is characterized by a ^{29}Si MAS-NMR band located at −85.51 (Figure 11b, Table 6) and related to Q^4 (4Al) sites. These data are consistent with the findings of Stebbins *et al.* (1986) who also reported the presence of another secondary peak at −93.9 ppm for a $KAlSiO_4$-01 grown by high-temperature sintering of oxides and two other secondary peaks for a $KAlSiO_4$-01 obtained after thermal treatment of kalsilite.

CONCLUSIONS

The results of the present study have proven that the reaction of kaolin with potassium carbonate leads to the formation of kaliophilite H2 and that this is indeed a metastable phase. The evolution of this phase was followed over time and allowed the authors to identify the stable phases.

In particular, crystallization of kalsilite and of $KAlSiO_4$-01 as isolated phases was achieved after 10 days and 5 days, at 700 and 800ºC, respectively. In other studies (*e.g.* Gorgeu, 1887; Heller-Kallai and Lapides, 2003), $KAlSiO_4$ minerals were synthesized starting from a natural kaolinitic precursor; thermal activation of kaolinite with K_2CO_3 at 700ºC for 1 h gave kaliophilite H2 as the final product (Heller-Kallai and Lapides, 2003). The syntheses presented here were performed over long periods compared with the experi-

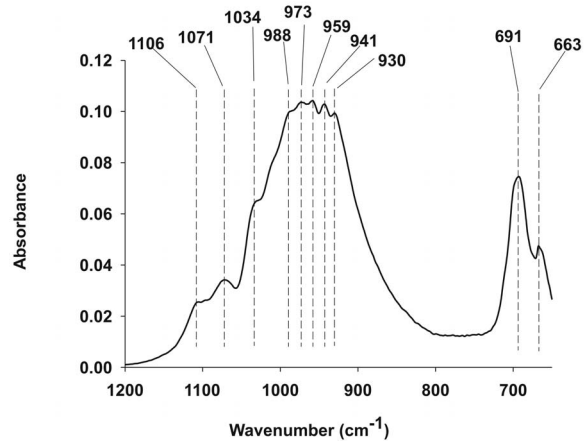

Figure 10. IR spectrum of synthesis run 2; sample at 5 days.

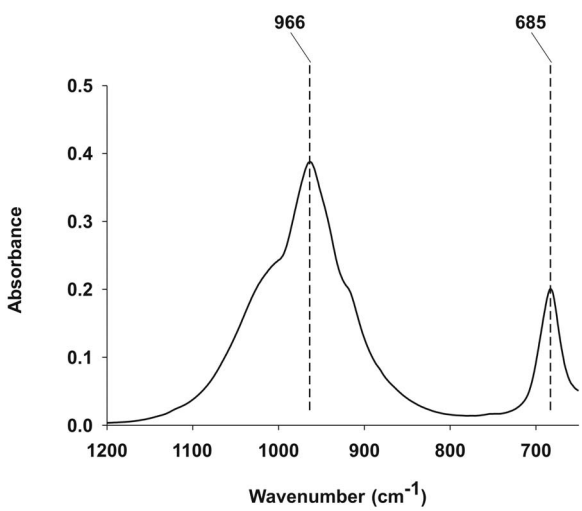

Figure 9. IR spectrum of synthesis run 1; sample at 10 days.

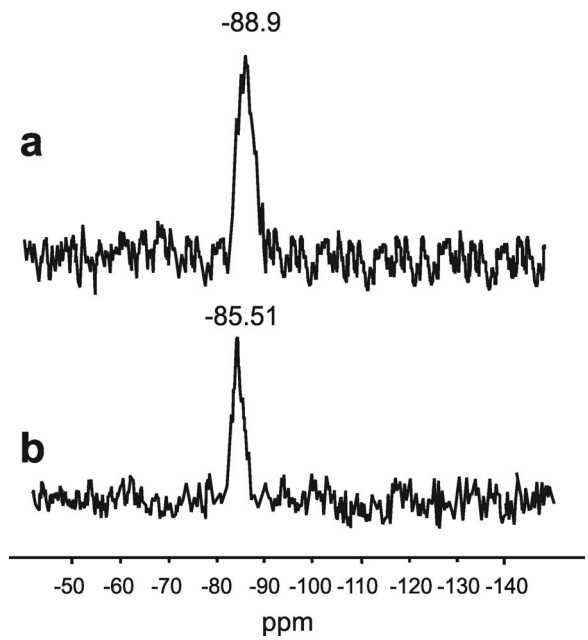

Figure 11. ^{29}Si MAS-NMR spectra: (a) sample at 10 days of synthesis run 1; and (b) sample at 5 days of synthesis run 2.

Table 5. Asymmetric stretch of inner bonds and symmetric stretch of external Si−O bonds for samples of synthesis runs 1 (10 days) and 2 (5 days).

Sample	Symmetric Si−O	Assymetric Si−O
Synthesis run 700ºC		
10 days	966	685
(*) Kalsilite	1037−985	684
(**) Kalsilite	1030−983	688
Synthesis run 800ºC		
5 days	1106−1071−1034−988−973−959−941−930	691−663
$KAlSiO_4$-01 (***)	1100−1070−1040−990−940−880	700−665

*Becerro *et al.* (2009); **Henderson and Taylor (1988); and ***Dimitrijevic and Dondur (1995).

Table 6. ^{29}Si chemical shift (ppm) for synthesis runs 1 and 2.

Sample	^{29}Si Chemical shift (ppm)
Run synthesis 1	
10 days	−88.9
(*) Kalsilite	−89.1
(**) Synt. kalsilite	−89.63
(***) kalsilite	−88.8, (−94.0)
Run synthesis 2	
5 days	−85.51
(***) $KAlSiO_4$-01	−85.6, −88.8, (−92.0, −97.0)

*Becerro *et al.* (2009); **Dimitrijevic and Dondur (1995); and ***Stebbins *et al.* (1986).

ments conducted in the other studies (*e.g.* Gorgeu, 1887; Heller-Kallai and Lapides, 2003) and illustrated the phase transitions of kaliophilite H2 during a specific time interval.

Detailed characterization of the products synthesized found that the chemical-physical, morphological, and spectroscopic characteristics of the experimental products are comparable with those reported in the literature for the same minerals synthesized using different methods. In particular, the QPA analyses indicated a high purity for the minerals synthesized and this allows for industrial application.

ACKNOWLEDGMENTS

The authors acknowledge the technical staff at the University of Barcelona for their help during the development of the work. This is a contribution of the Spanish MICCIN PROJECT CGL2011-28022.

REFERENCES

Akokelar, D., Chaffee, A., and Howe, R.F. (1997) The transformation of kaolin to low-silica X zeolite. *Zeolites*, **19**, 359−365.

Andou, Y. and Kawahara, A. (1984) The refinement of the structure of synthetic kalsilite. *Mineralogical Journal*, **12**, 153−61.

Aulinas, M., Gimeno, D., Fernandez-Turiel, J.L., Font, L., Perez-Torrado, F.J., Rodriguez-Gonzalez, A., and Novell, G.M. (2010) Small-scale mantle heterogeneity on the source of the Gran Canaria (Canary Islands) Pliocene−Quaternary magmas. *Lithos*, **119**, 377−392.

Aznar, A.J. and La Iglesia, A. (1985) Obtención de zeolitas a partir de arcillas aluminosas españolas. *Boletín Geologíco y Minero*, **96**, 541−549.

Becerro, A.I. and Mantovani, M. (2009) Hydrothermal synthesis of kalsilite: a simple and economical method. *Journal of the American Ceramic Society*, **92**, 2204−2206.

Becerro, A.I., Escudero, A., and Mantovani, M. (2009) The hydrothermal conversion of kaolinite to kalsilite: influence of time, temperature, and pH. *American Mineralogist*, **94**, 1672−1678.

Bogdanoviciene, I., Jankeviciute, A., Pinkas, J., Beganskiene, A., and Kareiva, A. (2007) Sol-gel synthesis and characterization of kalsilite-type alumosilicates. *Materials Science (Medžiagotyra)*, **13** (3), 1392−1320.

Bogdanoviciene, I., Jankeviciute, A., Pinkas, J., Beganskiene, A., and Kareiva, A. (2008) Study of alumosilicate porcelains: sol-gel preparation, characterization and erosion evaluated by gravimetric method. *Materials Research Bulletin*, **43**, 2998−3007.

Cheng, H., Liu, Q., Zhang, J., and Frost, R.L. (2010a) Delamination of kaolinite-potassium acetate intercalates by ball-milling. *Journal of Colloid and Interface Science*, **348**, 355−359.

Cheng, H., Liu, Q., Zhang, J., and Frost, R.L. (2010b) A spectroscopic comparison of selected Chinese kaolinite, coal bearing kaolinite and halloysite a mid-infrared and near−infrared study. *Spectrochimica Acta Part A: Molecular and Biomolecular Spectroscopy*, **77**, 856−861.

Cook, L.P., Roth, R.S., Parker, H.S, and Negas, T. (1977) The system K_2O-Al_2O_3-SiO_2. Part 1. Phases on the $KAlSiO_4$–$KAlO_2$ join. *American Mineralogist*, **62**, 1180−90.

Demortier, A., Gobeltz, N., Lelieur, J.P., and Duhayon, C. (1999) Infrared evidence for the formation of an intermediate compound during the synthesis of zeolite Na-A from metakaolin. *International Journal of Inorganic Materials*, **1**, 129−134.

Dimitrijevic, R. and Dondur, V. (1995) Synthesis and characterization of $KAlSiO_4$ polymorphs on the SiO_2-$KAlO_2$ join. II. The end-member of ANA-type zeolite framework. *Journal of Solid State Chemistry*, **115**, 214−224.

Dollase, W.A. and Freeborn, W.P. (1977) The structure of $KAlSiO_4$ with $P6_3mc$ symmetry. *American Mineralogist*, **62**, 336−340.

Fernandez-Turiel, J.L., Gimeno, D., Rodríguez, J.J., Carnicero, M., and Valero, F. (2003) Spatial and seasonal water quality in a Mediterranean catchment: the Llobregat river (NE Spain). *Environmental Geochemistry and Health*, **25**, 253−474.

Frost, R.L., Locos, O.B., Kristof, J., and Kloprogge, J.T. (2001a) Infrared spectroscopic study of potassium and cesium acetate-intercalated kaolinites. *Vibrational Spectroscopy*, **26**, 33–42.

Frost, R.L., Makó, É., Kristóf, J., Horváth, É., and Kloprogge, J.T. (2001b) Modification of kaolinite surfaces by mechanochemical treatment. *Langmuir*, **17**, 4731–4738.

Gorgeu, A. (1887) Action du kaolin sur plusieurs composés alkalins: silicates doubles d'alumine et de potasse ou de soude. *Annales de Chimie et de Physique, 2ème séries*, X, 145–166, Masson, Paris.

Gregorkiewitz, M., Li, Y., White, T.J., Withers, R.L., and Sobrados, I. (2008) The structure of ''orthorhombic'' $KAlSiO_4$-01: evidence for Al-Si order from MAS NMR data combined with Rietveld refinement and electron microscopy. *The Canadian Mineralogist*, **46**, 1511–1526.

Gualtieri, A.F. (2000) Synthesis of sodium zeolites from a natural halloysite. *Physics and Chemistry of Minerals*, **28**, 719–728.

Gualtieri, A., Norby, P., Artioli, G., and Hanson J. (1997) Kinetics of formation of zeolite Na-A (LTA) from natural kaolinites. *Physics and Chemistry of Minerals*, **24**,191–199.

Hamilton, D.L. and Henderson, C.N.B. (1968) The preparation of silicate compositions by a gelling method. *Mineralogical Magazine*, **36**, 832–838.

Heller-Kallai, L. and Lapides, I. (2003) Thermal reactions of kaolinite with potassium carbonate. *Journal of Thermal Analysis and Calorimetry*, **71**, 689–698.

Heller-Kallai, L. and Lapides, I. (2007) Reactions of kaolinites and metakaolinites with NaOH – comparison of different samples (Part 1). *Applied Clay Science*, **35**, 99–107.

Henderson, C.M.B and Taylor, D. (1988) The structural behaviour of the nepheline family: (3) Thermal expansion of kalsilite. *Mineralogical Magazine*, **52**, 708–711.

Hovis, G.L., Spearing, D.R., Stebbins, J.F, Roux, J., and Clare, A. (1992) X-ray powder diffraction and ^{23}Na, ^{27}Al and ^{29}Si MAS-NMR investigation of nepheline–kalsilite crystalline solutions. *American Mineralogist*, **77**, 19–29.

Kawahara, A., Andou, Y., Marumo, F., and Okomo, M. (1987) The crystal structure of high temperature form of kalsilite ($KAlSiO_4$) at 950ºC. *Mineralogical Journal*, **13**, 260–270.

Kopp, O.C., Harris, L.A., and Clark, G.W. (1961) The hydrothermal conversion of muscovite to kalsilite and an iron-rich mica. *American Mineralogist*, **46**, 719–727.

Kosanović, C., Subotic, B., Šmit, I., and Čižmek, A. (1997) Study of structural transformations in potassium-exchanged zeolite A induced by thermal and mechanochemical treatments. *Journal of Materials Science*, **32**, 73–78.

Kremenović, A., Lazic, B., Krüger, H., Tribus, M., and Vulić, P. (2013) Monoclinic structure and nonstoichiometry of "$KAlSiO_4$-01". *Acta Crystallographica*, **C69**, 334–336.

Larson, A.C. and Von Dreele, R.B. (1997) Los Alamos National Laboratory report: *Document Laur* 86-748.

Li, Ying, Laursen, K., White, T.J., and Gregorkievitz, M. (2003) The crystal chemistry and microstructure of fluidised bed incinerator clinker tridymite. *Journal of Material and Engineering*, **14**, 119–125.

Liou, C.L., Komarneni, S., and Roy, R. (1994) Seeding effect on crystallization of $KAlSi_3O_8$, $RbAlSi_3O_8$ and $CsAlSi_3O_8$ gels and glasses. *Journal American Ceramic Society*, **77**, 3105–3112.

Merlino, S. (1984) Feldspathoids: their average and real structures. Pp. 435–470 in: *Feldspars and Feldspathoids* (W.L. Brown, editor). NATO ASI Series C, Vol. **137**. Reidel Publishers, Dordrecht, The Netherlands.

Novembre, D., Di Sabatino, B., and Gimeno, D. (2005) Synthesis of Na-A zeolite from 10 Å halloysite and a new crystallization kinetic model for the transformation of Na-A into HS zeolite. *Clays and Clay Minerals*, **53**, 28–36.

Novembre, D., Gimeno, D., Pasculli, A., and Di Sabatino, B. (2010) Synthesis and characterization of sodalite using natural kaolinite: an analytical and mathematical approach to simulate the loss in weight of chlorine during the synthesis process. *Fresenius Environmental Bulletin*, **19**, 1109–1117.

Novembre, D., Di Sabatino, B., Gimeno, D., and Pace, C. (2011) Synthesis and characterization of Na-X, Na-A, hydroxysodalite and Na-P zeolites from metakaolinite, *Clay Minerals*, **46**, 336–354.

Novembre, D., Pace, C., and Gimeno, D. (2014) Synthesis and characterization of K-F and W merlinoite-type zeolites using a diatomite precursor. *Mineralogical Magazine*, **78**, 1209–1225.

Novembre, D., Pace, C., and Gimeno, D. (2017a) Synthesis and characterization of wollastonite-2*M* by using a diatomite precursor. *Mineralogical Magazine*, https://dx.doi.org/10.1180/minmag.2017.081.025.

Novembre, D., Gimeno, D., d'Alessandro, N. and Tonucci, L. (2017b) Hydrothermal synthesis and characterization of kalsilite by using a kaolinitic rock (Sardinia, Italy) and its application in the production of biodiesel. *Mineralogical Magazine*, https://doi.org/10.1180/minmag.2017.081.080.

Okamoto, Y. (1997) Structural modification of $KAlSiO_4$ minerals. *Okayama University Earth Science Reports*, **4**, 41–72.

Okamoto, Y. and Kawahara, A. (1996) Interpretation of the crystal structure of synthetic kaliophilite from the domain structure of kalsilite. *Okayama University Earth Science Reports*, **3**, 57–64.

Ota, T., Takebayashi, T., Takahashi, M., and Hikichi, Y. (1996) High thermal expansion $KAlSiO_4$ ceramic. *Journal of Materials Science*, **31**, 1431–1433.

Pasculli, A. and Novembre, D. (2012) A phenomenological-mathematical approach in simulating the loss in weight of chlorine during sodalite synthesis. *Computers and Geosciences*, **42**, 110–117.

Perrotta, A.J. and Smith, J.V. (1965) The crystal structure of kalsilite $KAlSiO_4$. *Mineralogical Magazine*, **35**, 588–95.

Qtaitat, M.A. and Al-Trawneh, I.N. (2005) Characterization of kaolinite of the Baten El-Ghoul region/south Jordan by infrared spectroscopy. *Spectrochimica Acta*, **(A) 61**, 1519–1523.

Rigby, G.R. and Richardson, H.M. (1947) The occurrence of artificial kalsilite and allied potassium aluminum silicates in blast furnace linings. *Mineralogical Magazine*, **28**, 75–88.

Ríos, C.A., Williams, C.D., and Fullen, M.A. (2009) Nucleation and growth history of zeolite LTA synthesized from kaolinite by two different method. *Applied Clay Science*, **42**, 446–454.

Ríos, C.A. and Williams, C.D. (2010) Hydrothermal transformation of kaolinite in the system K_2O-SiO_2-Al_2O_3-H_2O. *Dyna*, **77**, 55–63.

Robert, J.L., Della Ventura, G., and Thauvin, G. (1989) The infrared OH-stretching region of synthetic richterites in the system Na_2O-K_2O-CaO-MgO-SiO_2-H_2O-HF. *European Journal of Mineralogy*, **1**, 203–211.

Rocha, J. and Klinowski, J. (1991) Synthesis of Zeolite Na-A from metakaolinite revisited. *Journal of the Chemical Society, Faraday Transactions*, **87**, 3091–3097.

Ruggieri, F., Fernandez-Turiel J.L., Saavedra, J., Gimeno D., Polanco, E., and Naranjo, J.A. (2011) Environmental geochemistry of recent volcanic ashes from Southern Andes. *Environmental Chemistry*, **8**, 236–247.

Sabine, P.A. and Young, B.R. (1975) Metamorphic processes at high temperature and low pressure: the petrogenesis of the metasomatized and assimilated rocks of Carneal, Co. Antrim. *Philosophical Transactions of the Royal Society of London, Series A, Mathematical and Physical Sciences*,

280, 225–269.

Sanhueza, V., Kelm, U., and Cid, R. (1999) Synthesis of molecular sieves from Chilean kaolinites: I. Synthesis of Na A type zeolites. *Journal of Chemical Technology and Biotechnology*, **74**, 358–363.

Smith, J.V. and Tuttle, O.F. (1957) The nepheline-kalsilite system: 1. X-ray data for the crystalline phases. *American Journal of Science*, **255**, 282–305.

Stebbins, J.F., Murdoch, J.B., Carmichael I.S.E., and Pines, A. (1986) Defects and short-range order in nepheline group minerals: a Silicon-29 nuclear magnetic resonance study. *Physics and Chemistry of Minerals*, **13**, 371–381.

Toby, B.H. (2001) EXPGUI, a graphical user interface for GSAS. *Journal of Applied Crystallography*, **34**, 210–213.

Tuttle, O.F. and Smith, J.V. (1958) The nepheline-kalsilite system II: phase relations. *American Journal of Science*, **256**, 571–589.

Wen, G., Yan, Z., Sinth, M., Zhang, P., and Wen, B. (2010) Kalsilite based heterogeneous catalyst for biodiesel production. *Fuel*, **89**, 2163–2165.

Zhang, Y., Lv, M., Chen, D., and Wu, J. (2007) Leucite crystallization kinetics with kalsilite as a transition phase. *Materials Letters*, **61**, 2978–2981.

Zhao, H., Deng, Y., Harsh, J.B., and Flury, M. (2004) Alteration of kaolinite to cancrinite and sodalite by simulated Hanford tank waste and its impact on cesium retention. *Clays and Clay Minerals*, **52**, 1–13.

(*Received 2 November 2016; revised 27 November 2017; Ms. 1147; AE: J. Brendlé-Miehé*)